

2007

# Development of Method for Synthesis of Pt–Co Cathode Catalysts for PEM Fuel Cells

Xuguang Li

*University of South Carolina - Columbia*

Héctor R. Colón-Mercado

*University of South Carolina - Columbia*

Gang Wu

*University of South Carolina - Columbia*

Jong-Won Lee

*University of South Carolina - Columbia*

Branko N. Popov

*University of South Carolina - Columbia, popov@engr.sc.edu*

Follow this and additional works at: [https://scholarcommons.sc.edu/eche\\_facpub](https://scholarcommons.sc.edu/eche_facpub)

 Part of the [Chemical Engineering Commons](#)

---

## Publication Info

*Electrochemical and Solid-State Letters*, 2007, pages B201-B205.

© The Electrochemical Society, Inc. 2007. All rights reserved. Except as provided under U.S. copyright law, this work may not be reproduced, resold, distributed, or modified without the express permission of The Electrochemical Society (ECS). The archival version of this work was published in *Electrochemical and Solid-State Letters*.

<http://www.electrochem.org/>

Publisher's link: <http://dx.doi.org/10.1149/1.2777009>

DOI: 10.1149/1.2777009



## Development of Method for Synthesis of Pt–Co Cathode Catalysts for PEM Fuel Cells

Xuguang Li,\* Héctor R. Colón-Mercado, Gang Wu,  
Jong-Won Lee, and Branko N. Popov\*\*<sup>z</sup>

Center for Electrochemical Engineering, Department of Chemical Engineering, University of South Carolina, Columbia, South Carolina 29208, USA

A procedure was developed to synthesize a platinum–cobalt (Pt–Co) alloy electrocatalyst for oxygen reduction using Co/C composite as a support. The Pt–Co/C catalysts were synthesized through: (i) chemical oxidation of carbon black, (ii) Co deposition on the oxidized carbon using a chelation method, (iii) chemical treatment in an acidic medium to remove excess of Co on the carbon surface, (iv) Pt deposition onto the Co/C support, and (v) postheat treatment to form the Pt–Co alloy catalyst. The synthesized Pt–Co/C catalyst showed improved activity and long-term stability in polymer electrolyte membrane (PEM) fuel cells when compared with a conventional Pt–Co/C catalyst. The electron probe microanalysis combined with scanning electron microscopy indicated that the Co content in the alloy catalyst remains stable without poisoning of the electrolyte membrane during long-term operation.

© 2007 The Electrochemical Society. [DOI: 10.1149/1.2777009] All rights reserved.

Manuscript submitted July 16, 2007; revised manuscript received August 7, 2007. Available electronically September 4, 2007.

Alloying platinum with transition metals increases a catalytic activity of Pt-based catalyst for the oxygen reduction reaction in polymer electrolyte membrane (PEM) fuel cells. According to literature, the observed increase of catalytic activity results from: (i) increase in the resistance to particle sintering, (ii) surface roughening due to removal of some alloying metal that increases the Pt surface area, (iii) preferential crystal orientation, and (iv) a more favorable Pt–Pt interatomic distance.<sup>1–6</sup>

Among various Pt alloy catalysts, Pt–Co is considered to be the most promising alloy catalyst due to its relatively high activity and stability in acidic environments. Conventional Pt–Co/C catalyst is prepared by depositing cobalt colloid onto a Pt/C catalyst from aqueous solutions of cobalt salt such as  $\text{Co}(\text{NO}_3)_2$  and  $\text{Co}(\text{SO}_4)_2$  (i.e., surface modification of Pt particles by Co), followed by postheat treatment at 700–1000°C under inert or reducing atmosphere.<sup>7–19</sup>

It has been reported that the alloying elements act as an anchor on the carbon support, thereby inhibiting the Pt migration and aggregation in the alloy catalysts.<sup>8,20</sup> However, even well-alloyed Co elements were found to leach out of Pt–Co alloy under acidic fuel cell environments, leaving a Pt-enriched surface.<sup>8</sup> Dissolution of Co elements from the alloy catalyst results in not only the loss of intrinsic catalytic activity, but also the poisoning of membrane electrode assembly (MEA) via ion exchange between Co ions and protonic sites in both Nafion membrane and the ionomer inside the catalyst layer. Consequently, these phenomena cause a significant degradation of long-term performance of PEM fuel cells.<sup>8</sup>

Our previous study demonstrated that highly active Co/C catalysts can be prepared through a chelation method, by supporting Co–N complexes on a carbon black followed by heat treatment at elevated temperatures.<sup>21–23</sup> Oxygen functional groups introduced on the carbon surface with an acid treatment improved the dispersion of Co–N complexes, resulting in enhanced catalytic activity and selectivity towards four-electron oxygen reduction. In this work, a methodology was developed to synthesize the Pt–Co/C catalyst with high activity and stability, using the Co/C composite as a support. The Co/C was synthesized using a chelation method developed by our group, and then treated in an acidic medium to remove excess Co on the carbon surface. Next, Pt was deposited onto the Co/C support, followed by postheat treatment to form the Pt–Co alloy catalyst. The

catalytic activity and stability of Pt–Co/C catalyst were evaluated in PEM fuel cells and compared with those of a conventional Pt–Co/C catalyst currently in use in MEA.

### Experimental

**Preparation of cobalt/carbon composite support.**—As-received carbon black (Ketjen Black EC 300J) was treated with 9.8 M  $\text{HNO}_3$  solution at 80°C for 7 h under refluxing conditions, in order to introduce oxygen functional groups onto the carbon surface. The oxidized carbon specimen was rinsed with deionized water, followed by drying under vacuum at 80°C.

A cobalt–nitrogen chelate complex ( $\text{CoN}_x$ ) was deposited onto the oxidized carbon using  $\text{Co}(\text{NO}_3)_2$  (Aldrich, 98%) and ethylene diamine ( $\text{H}_2\text{NCH}_2\text{CH}_2\text{NH}_2$ ) as Co and N precursors, respectively.<sup>21</sup> A desired amount of ethylene diamine was added slowly into 0.015 M  $\text{Co}(\text{NO}_3)_2$  solution in ethanol, followed by the addition of the oxidized carbon powder under stirring conditions. The molar Co:N ratio in the reaction mixture was maintained at 1:16. The reaction mixture was refluxed at 85°C for 4 h, followed by drying under vacuum at 80°C. The resulting Co-deposited carbon was subjected to heat treatment in an argon atmosphere at 700°C and at 8.8 MPa for 3 h. The heat-treated Co/C sample was treated with 0.5 M  $\text{H}_2\text{SO}_4$  at 25°C for 2 h to remove excess Co on the carbon surface.

**Platinum deposition on cobalt/carbon support.**—4.0 mM  $\text{H}_2\text{PtCl}_6$  and 0.27 M HCl solutions were mixed with deionized water containing the Co/C support; 2.0 M sodium formate ( $\text{HCOONa}$ ) solution was added slowly to the reaction mixture, followed by refluxing at 80°C for 20 h. The resulting Pt–Co/C sample was rinsed with deionized water, and then was dried under vacuum at 80°C for 12 h. Finally, the Pt–Co/C catalyst was heat treated in an argon atmosphere at 800°C for 1 h.

**Performance test of membrane-electrode assemblies.**—The cathode catalyst ink was prepared by ultrasonically blending Pt–Co/C catalyst powder with Nafion solution (5 wt %) and isopropyl alcohol for 4 h. The catalyst ink was then sprayed onto a gas diffusion layer (GDL) (ELAT LT 1400W, E-TEK) until a total metal loading of 0.4 mg  $\text{cm}^{-2}$  has been achieved. A commercially available catalyzed GDL (LT140EW low temperature GDE microporous layer, E-TEK) was used as the anode for all fuel cell tests. The anode catalyst was 30 wt % Pt/C and the Pt loading was 0.5 mg  $\text{cm}^{-2}$ . A thin layer of Nafion (0.4 mg  $\text{cm}^{-2}$ ) was coated on both the cathode and anode surfaces. The Nafion-coated anode and cathode were hot pressed to a Nafion 112 membrane at 140°C and at 534 kPa for 3 min. The geometric area of the MEA used was 5  $\text{cm}^2$ .

\* Electrochemical Society Student Member.

\*\* Electrochemical Society Active Member.

<sup>z</sup> E-mail: popov@engr.sc.edu

**Table I. Compositions of the leached Co/C support and the heat-treated Pt–Co/C catalyst determined by ICP-MS.**

Sample	Concentration (wt %)		
	C	Co	Pt
Co/C (after leaching in H <sub>2</sub> SO <sub>4</sub> )	97.0	3.0	...
Pt–Co/C (after heat treatment at 800°C)	80.5	2.7	16.8

The MEA tests were carried out in a single cell with serpentine flow channels. Pure H<sub>2</sub> gas humidified at 77°C and pure O<sub>2</sub> gas humidified at 75°C were supplied with a flow rate of 150 cm<sup>3</sup> min<sup>-1</sup> to the anode and cathode compartments, respectively. Polarization experiments were conducted with a fully automated test station (Fuel Cell Technologies Inc.) at 75°C and at ambient pressure. In order to evaluate the stability of catalyst and MEA, galvanostatic potential transient technique was performed by applying a constant current density of 1.0 A cm<sup>-2</sup>. Polarization measurements were periodically carried out to determine the MEA performance during stability testing.

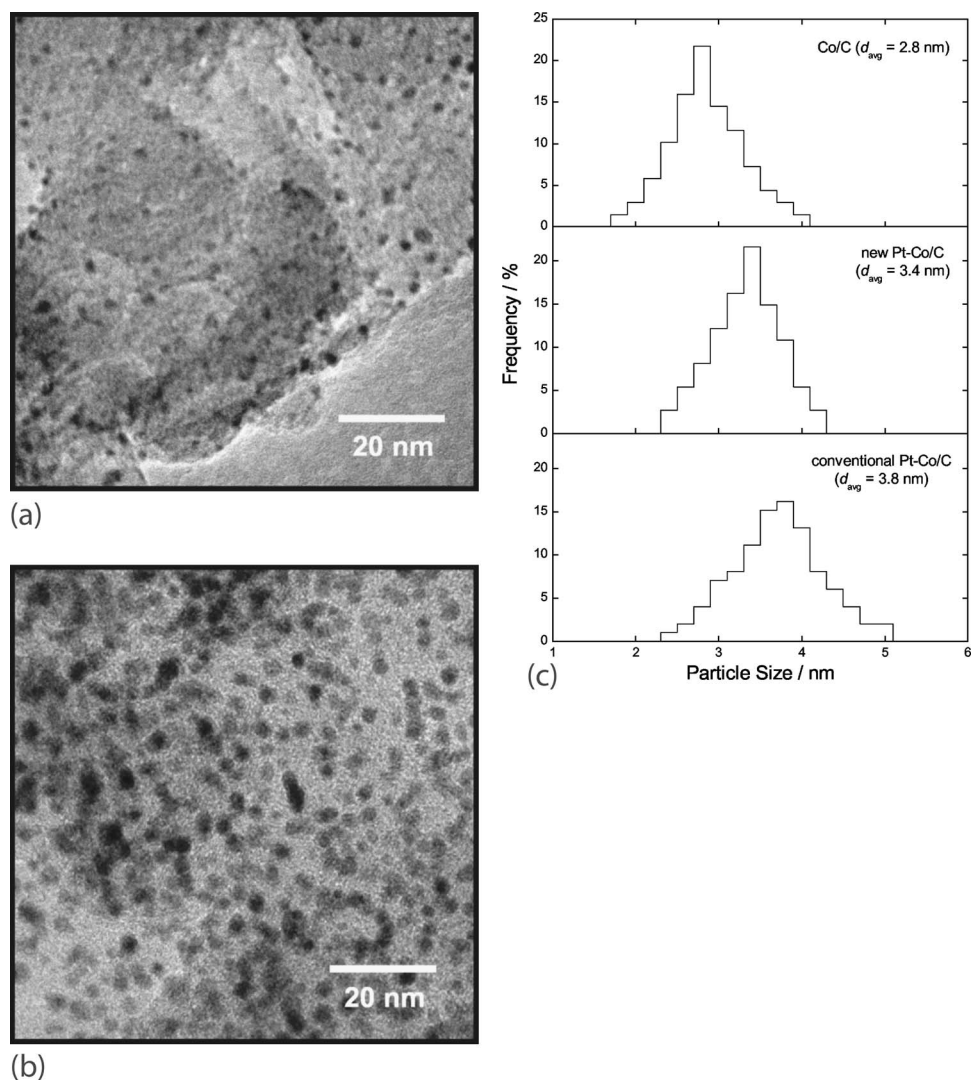
**Materials characterizations.**— Inductively coupled plasma-mass spectroscopy (ICP-MS) was conducted with an SCIEX ELAN DRCE ICP-MS system (Perkin-Elmer) to analyze the catalyst com-

position. In order to identify the crystal structure of the synthesized catalyst, powder X-ray diffraction (XRD) patterns were recorded with a Rigaku 405S5 using a Cu K $\alpha$  radiation at a scan rate of 1.5° min<sup>-1</sup>. To determine the particle size of the catalyst, transmission electron microscopy (TEM) was carried out using a high-resolution JEOL 2010F TEM system operated with LaB<sub>6</sub> filament at 200 kV. Backscattering scanning electron microscopy (BSEM) (ESEM FEI Quanta 200) and electron probe microanalysis (EPMA) (Cameca SX 50) were performed to determine the cathode catalyst layer thickness and the concentration profiles of Pt and Co across the MEA.

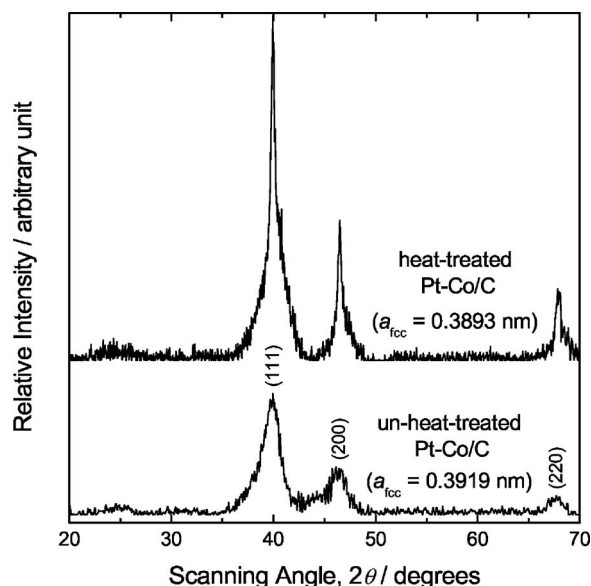
## Results and Discussion

Table I summarizes the compositions of the leached Co/C support and the heat-treated Pt–Co/C catalyst analyzed by ICP-MS technique. The Co concentration in the leached Co/C support was 3.0 wt %. The Pt–Co/C catalyst consisted of 16.8 wt % Pt and 2.7 wt % Co (i.e., the total metal loading of 19.5 wt %). The ICP analysis indicates no loss of Co during electroless deposition of Pt from acidic H<sub>2</sub>PtCl<sub>6</sub>–HCl solution.

Figures 1a and b present the TEM images of the leached Co/C support and the heat-treated Pt–Co/C catalyst, respectively. The metal particle size distributions (PSDs) determined from the TEM images are shown in Fig. 1c along with the data for a conventional Pt–Co/C catalyst (20 wt % Pt<sub>3</sub>Co<sub>1</sub>/C, E-TEK). As shown in Fig. 1a and c, Co particles are highly dispersed on the oxidized carbon black



**Figure 1.** TEM images of (a) the leached Co/C support and (b) the heat-treated Pt–Co/C catalyst, and (c) metal particle size distributions determined from the TEM images.



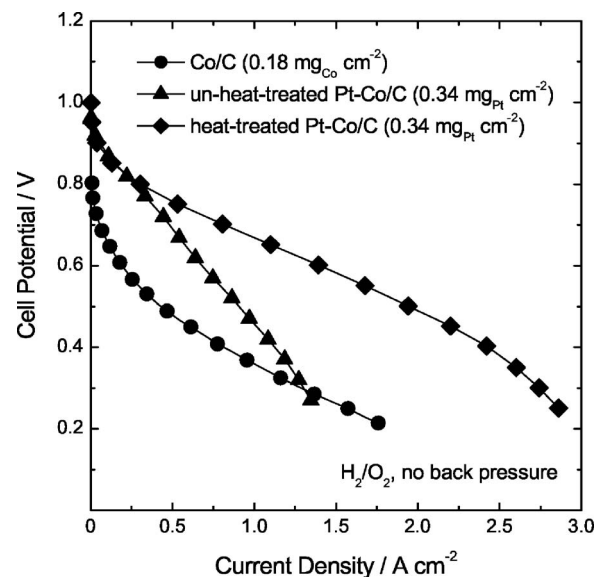
**Figure 2.** Powder XRD patterns of the unheat-treated and heat-treated Pt-Co/C catalysts. The fcc lattice parameters,  $a_{\text{fcc}}$ , determined from the XRD data are given in the figure.

showing a narrow size distribution, and the average particle size was determined to be approximately 2.8 nm. The synthesis of Co/C support involves carbon oxidation in  $\text{HNO}_3$  solution as described in the preceding section. Our previous study showed that quinone-type oxygen groups formed onto the carbon surface during carbon oxidation improve the dispersion of Co particles on the carbon black by facilitating the adsorption of Co-ethylene diamine complex.<sup>21</sup> Upon Pt deposition on the Co/C support, the average particle size slightly increased to 3.4 nm, while the shape of PSD curve remained nearly unchanged. No agglomeration of catalyst particles on the support is observed in Fig. 1b. The Pt-Co/C catalyst prepared in this study shows a smaller mean particle size and a narrower PSD, as compared with the conventional catalyst ( $\sim 3.8$  nm).

Figure 2 presents the powder XRD patterns of the unheat-treated and heat-treated Pt-Co/C catalysts. The XRD pattern of the unheat-treated Pt-Co/C catalyst shows the characteristic diffraction peaks of the face centered cubic structure at  $2\theta = 39.7, 46.2,$  and  $67.5^\circ$  that correspond to (111), (200), and (220) planes, respectively. The diffraction peaks became sharper upon postheat treatment, indicating increased crystallite (or particle) sizes. Further, the diffraction peaks shifted slightly towards higher Bragg angles, which indicates a decreased lattice constant due to the formation of Pt-Co alloy.<sup>9</sup> In fact, the fcc lattice parameters of the unheat-treated and heat-treated Pt-Co catalysts were estimated to be 0.3919 and 0.3893 nm, respectively, from the XRD data in Fig. 2.

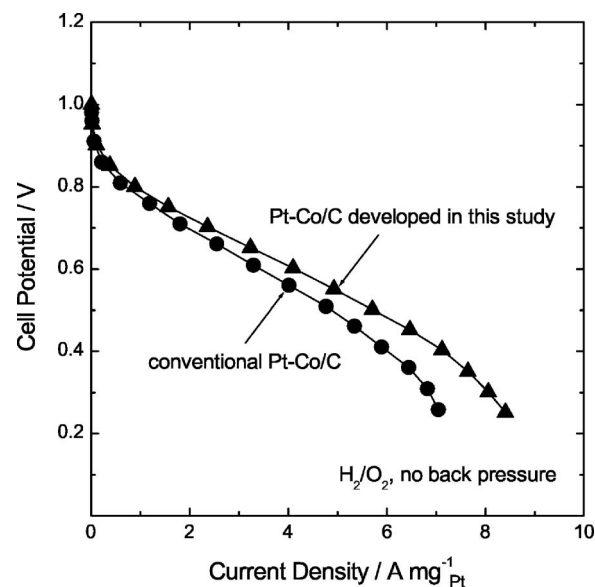
Figure 3 shows polarization curves of the PEM fuel cells prepared with three different catalysts namely: (i) Co/C composite, (ii) unheat-treated Pt-Co/C, and (iii) heat-treated Pt-Co/C. The fuel cell with the Co/C catalyst exhibited current densities of  $0.78 \text{ A cm}^{-2}$  at 0.4 V and  $1.76 \text{ A cm}^{-2}$  at 0.2 V at ambient pressure. The synthesis route based on carbon oxidation and chelation produces Co/C with a superior catalytic performance than those previously reported.<sup>7</sup> Besides the fact that both Pt-Co/C catalysts contains the same amounts of Pt and Co, the heat-treated catalyst exhibits much higher activity, e.g.,  $1.40 \text{ A cm}^{-2}$  at 0.6 V, when compared with the unheat-treated catalyst ( $0.67 \text{ A cm}^{-2}$ ). An enhanced activity of the heat-treated Pt-Co/C catalyst results from the alloy formation of Pt and Co, as indicated by the XRD analysis in Fig. 2.

Figure 4 compares polarization curves of the PEM fuel cells with the Pt-Co/C catalyst developed in this study and a conventional Pt-Co/C catalyst (20 wt %  $\text{Pt}_3\text{Co}_1$ , E-TEK). The Pt-Co loading in



**Figure 3.** Polarization curves of the PEM fuel cells prepared with (i) Co/C, (ii) unheat-treated Pt-Co/C, and (iii) heat-treated Pt-Co/C. The experiments were performed under the following conditions: (i) Pt loading on the anode =  $0.5 \text{ mg cm}^{-2}$ , (ii)  $\text{H}_2$  flow rate =  $150 \text{ cm}^3 \text{ min}^{-1}$ , (iii)  $\text{O}_2$  flow rate =  $150 \text{ cm}^3 \text{ min}^{-1}$ , and (iv) cell temperature =  $75^\circ\text{C}$ .

the MEA was maintained at  $0.4 \text{ mg cm}^{-2}$  for both catalysts. The measured current density was normalized with respect to the Pt loading in the MEA because of a small difference in Pt concentrations in the two catalysts. The polarization measurements clearly show that the new Pt-Co/C catalyst leads to a superior fuel cell performance over the conventional catalyst over the whole potential range. At 0.6 V, the current density for the new Pt-Co/C catalyst was  $4.2 \text{ A mg}_{\text{Pt}}^{-1}$  in comparison to  $3.3 \text{ A mg}_{\text{Pt}}^{-1}$  for the conventional catalyst, i.e., a performance increase of approximately 26%. Based



**Figure 4.** Polarization curves of the PEM fuel cells with the Pt-Co/C catalyst developed in this study and the conventional Pt-Co/C catalyst. The experiments were performed under the following conditions: (i) Pt loading on the anode =  $0.5 \text{ mg cm}^{-2}$ , (ii) Pt-Co loading on the cathode =  $0.4 \text{ mg cm}^{-2}$ , (iii)  $\text{H}_2$  flow rate =  $150 \text{ cm}^3 \text{ min}^{-1}$ , (iv)  $\text{O}_2$  flow rate =  $150 \text{ cm}^3 \text{ min}^{-1}$ , and (v) cell temperature =  $75^\circ\text{C}$ . The measured current density was normalized with respect to the Pt loading in the MEA.

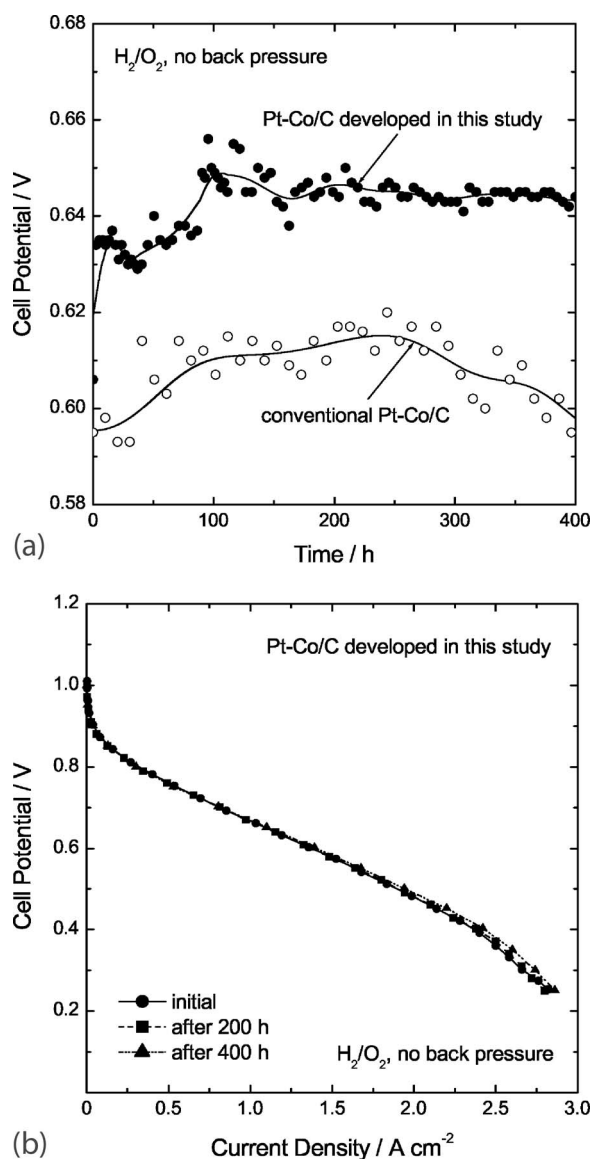


**Figure 5.** (a) Potential transients of the PEM fuel cells measured at a constant current density of  $1.0 \text{ A cm}^{-2}$  using the Pt-Co/C catalyst synthesized in this study and the conventional Pt-Co/C catalyst, and (b) polarization curves for the new Pt-Co/C catalyst measured during stability testing. The experiments were performed under the following conditions: (i) Pt loading on the anode =  $0.5 \text{ mg cm}^{-2}$ , (ii) Pt-Co loading on the cathode =  $0.4 \text{ mg cm}^{-2}$ , (iii)  $\text{H}_2$  flow rate =  $150 \text{ cm}^3 \text{ min}^{-1}$ , (iv)  $\text{O}_2$  flow rate =  $150 \text{ cm}^3 \text{ min}^{-1}$ , and (v) cell temperature =  $75^\circ\text{C}$ .

on the above results, the improved catalytic activity of the new Pt-Co/C catalyst over the conventional catalyst may be attributed to (i) a more uniform dispersion of smaller catalyst particles over the support (Fig. 2) and (ii) the high catalytic activity of Co/C composite used as a support (Fig. 3).

In order to address the stability of Pt-Co/C catalyst in PEM fuel cell, the galvanostatic potential transient technique was performed with a current density of  $1.0 \text{ A cm}^{-2}$  using  $\text{H}_2$  and  $\text{O}_2$ , and the polarization curves were periodically measured during stability testing. Figure 5a compares the potential transients of the PEM fuel cells with the new and conventional Pt-Co/C catalysts. The cell potential for the conventional Pt-Co/C catalyst started to decay after  $\sim 250 \text{ h}$  of continuous operation. For the new Pt-Co/C catalyst, on the other hand, the potential transient shows an initial potential increase, followed by a steady-state potential profile of  $\sim 0.65 \text{ V}$ . As

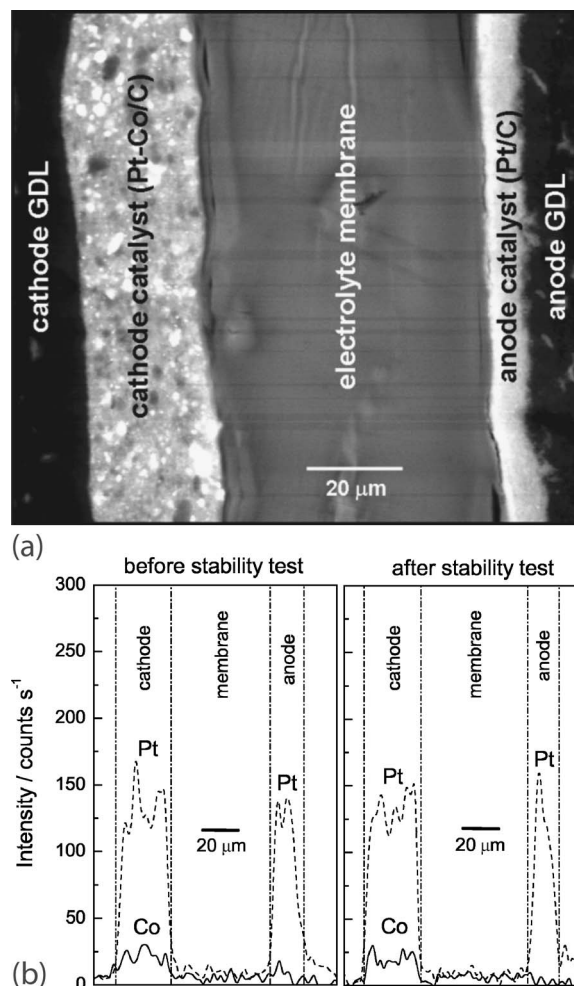


**Figure 6.** (a) BSEM images obtained from the cross sections of the fresh MEA with the Pt-Co/C catalyst developed in this study, and (b) concentration profiles of Pt and Co across the fresh MEA and the MEA subjected to 400 h of stability testing, obtained by EPMA cross section line scan.

shown in Fig. 5b, no degradation of fuel cell performance was observed when polarization curves were measured after 200 and 400 h of stability testing.

It has been reported that Co leaches out of Pt-Co alloy during fuel cell operation, since Co is thermodynamically unstable at PEM fuel cell potentials in acidic environments.<sup>7,8</sup> The polymer electrolyte membrane (Nafion) currently in use in MEA is very susceptible to contamination by Co ions dissolved from the alloy catalyst, due to the limited amount of protonic sites available in the membrane.<sup>7,24</sup> The MEA cross-sectional analysis by EPMA in our previous study confirmed a significant dissolution of Co from the commercial Pt-Co/C catalyst followed by diffusion into the membrane.<sup>8</sup> The membrane poisoning by dissolved Co elements resulted in a significant deterioration of long-term fuel cell performance.

Figure 6a presents the BSEM images obtained from the cross sections of the MEA prior to stability testing. The image shows the five distinctive layers: (i) cathode GDL, (ii) cathode Pt-Co/C catalyst layer, (iii) electrolyte membrane, (iv) anode Pt/C catalyst layer, and (v) anode GDL. The thickness of the cathode Pt-Co/C catalyst layer was  $\sim 26 \mu\text{m}$ . Figure 6b illustrates the concentration profiles of Pt and Co across the fresh MEA and the MEA subjected to stability testing for 400 h. The data were obtained by EPMA cross section line scan combined with the BSEM. Since there is no significant signal coming from Co in the membrane in the both MEAs,

the results indicate that Co remains stable in Pt–Co/C catalyst developed in this study.

The improved stability of Pt–Co/C developed at USC is due to the following: (i) the excess Co in the alloy has been removed by leaching the catalyst in H<sub>2</sub>SO<sub>4</sub> solution (only stable Co species remain in the carbon composite support); (ii) surface functional groups such as oxygen and nitrogen introduced during the preparation of the carbon composite support inhibit Co migration and dissolution; and (iii) interaction of Pt with Co/C at high temperature results in formation of a chemically and structurally stable Pt–Co/C alloy when compared with the conventional synthesis routes involving Co deposition on Pt/C.

### Conclusion

The Pt–Co cathode catalyst for PEM fuel cells was developed using a synthesis method involving the use of the Co/C composite as a support and the electroless deposition of Pt on Co/C. The heat treatment after the electroless Pt deposition led to the alloy formation of Pt and Co, resulting in a significant increase in the catalytic activity. The TEM analysis showed that the synthesized catalyst exhibits smaller particle sizes and more uniform distributions on the carbon, as compared with the conventional Pt–Co/C catalyst. The new Pt–Co/C catalyst showed improved activity and long-term stability in PEM fuel cells when compared with the conventional Pt–Co/C catalyst. The EPMA study combined with BSEM indicated that Co remains stable in the new alloy catalyst without poisoning the electrolyte membrane during stability testing.

### Acknowledgments

The financial support of the National Science Foundation Industry/University Cooperative Research for Fuel Cells at the University of South Carolina is gratefully acknowledged. The research on development of carbon composite support materials was supported by the Department of Energy (contract no. DE-FC36-03GO13108).

The University of South Carolina assisted in meeting the publication costs of this article.

### References

1. T. Toda, H. Igarashi, H. Uchida, and M. Watanabe, *J. Electrochem. Soc.*, **146**, 3750 (1999).
2. V. Jalan and E. J. Taylor, *J. Electrochem. Soc.*, **130**, 2299 (1983).
3. S. Mukerjee and S. Srinivasan, *J. Electroanal. Chem.*, **357**, 201 (1993).
4. M. T. Paffet, G. J. Beery, and S. Gottesfeld, *J. Electrochem. Soc.*, **135**, 1431 (1988).
5. N. M. Markovic and P. N. Ross, *Electrochim. Acta*, **45**, 4101 (2000).
6. S. Mukerjee, S. Srinivasan, M. P. Soriaga, and J. McBreen, *J. Electrochem. Soc.*, **142**, 1409 (1995).
7. H. A. Gasteiger, S. S. Kocha, B. Sompalli, and F. T. Waner, *Appl. Catal., B*, **56**, 9 (2005).
8. H. R. Colón-Mercado and B. N. Popov, *J. Power Sources*, **155**, 253 (2006).
9. E. Antolini, *Mater. Chem. Phys.*, **78**, 563 (2003).
10. P. Yu, M. Pemberton, and P. Plasse, *J. Power Sources*, **144**, 11 (2005).
11. T. R. Ralph and M. P. Hogarth, *Platinum Met. Rev.*, **46**, 3 (2002).
12. E. I. Santiago, L. C. Varanda, and H. M. Villullas, *J. Phys. Chem. C*, **111**, 3146 (2007).
13. S. J. Seo, H.-I. Joh, H. T. Kim, and S. H. Moon, *J. Power Sources*, **163**, 403 (2006).
14. E. Antolini, J. R. C. Salgado, and E. R. Gonzalez, *J. Power Sources*, **160**, 957 (2006).
15. J. N. Soderberg, A. H. C. Sirk, S. A. Campbell, and V. I. Birssa, *J. Electrochem. Soc.*, **152**, A2017 (2005).
16. V. Stamenkovic, T. J. Schmidt, P. N. Ross, and N. M. Markovic, *J. Phys. Chem. B*, **106**, 11970 (2002).
17. U. A. Paulus, A. Wokaun, G. G. Scherer, T. J. Schmidt, V. Stamenkovic, V. Radmilovic, N. M. Markovic, and P. N. Ross, *J. Phys. Chem. B*, **106**, 4181 (2002).
18. L. Xiong, A. M. Kannan, and A. Manthiram, *Electrochem. Commun.*, **4**, 898 (2002).
19. J. R. C. Salgado, E. Antolini, and E. R. Gonzalez, *J. Power Sources*, **141**, 13 (2005).
20. H. R. Colón-Mercado, H. Kim, and B. N. Popov, *Electrochem. Commun.*, **6**, 795 (2004).
21. N. P. Subramanian, S. P. Kumaraguru, H. Colón-Mercado, H. Kim, B. N. Popov, T. Black, and D. A. Chen, *J. Power Sources*, **157**, 56 (2006).
22. L. Liu, J.-W. Lee, and B. N. Popov, *J. Power Sources*, **162**, 1099 (2006).
23. L. Liu, H. Kim, J.-W. Lee, and B. N. Popov, *J. Electrochem. Soc.*, **154**, A123 (2007).
24. B. Smitha, S. Sridhar, and A. A. Khan, *J. Membr. Sci.*, **259**, 10 (2005).